

FOLD–SADDLE BIFURCATION IN NON–SMOOTH VECTOR FIELDS ON THE PLANE.

CLAUDIO A. BUZZI¹, TIAGO DE CARVALHO¹ AND
MARCO A. TEIXEIRA²

ABSTRACT. This paper presents results concerning bifurcations of $2D$ piecewise–smooth dynamical systems governed by vector fields. Generic three–parameter families of a class of Non–Smooth Vector Fields are studied and its bifurcation diagrams are exhibited. Our main results describe the unfolding of the so called *Fold – Saddle* singularity.

1. INTRODUCTION

The general purpose of this article is to present some aspects of the geometric and qualitative theory of a class of planar non–smooth systems. Our main concern is to discuss the behavior of such systems around typical singularities that appear generically in three–parameter families. We mention that certain phenomena in control systems, impact in mechanical systems and nonlinear oscillations are the main sources of motivation of our study concerning the dynamics of those systems that emerge from differential equations with discontinuous right–hand sides.

The codimension zero and codimension one singularities were discussed in [4] and [5] respectively. In [3] codimension two singularities were studied. The specific topic addressed in this paper is the complete characterization of the *Fold–Saddle bifurcation diagram*. Those papers give the necessary basis for the development of our approach.

Let $K \subseteq \mathbb{R}^2$ be a compact set and $\Sigma \subseteq K$ given by $\Sigma = f^{-1}(0)$, where $f : K \rightarrow \mathbb{R}$ is a smooth function having $0 \in \mathbb{R}$ as a regular value (i.e. $\nabla f(p) \neq 0$, for any $p \in f^{-1}(0)$) such that $\partial K \cap \Sigma = \emptyset$ or $\partial K \pitchfork \Sigma$. Clearly Σ is the separating boundary of the regions $\Sigma_+ = \{q \in K | f(q) \geq 0\}$ and $\Sigma_- = \{q \in K | f(q) \leq 0\}$. We can assume that Σ is represented, locally around a point $q = (x, y)$, by the function $f(x, y) = y$.

Designate by χ^r the space of C^r vector fields on K endowed with the C^r –topology with $r \geq 1$ or $r = \infty$, large enough for our purposes. Call

1991 *Mathematics Subject Classification*. Primary 34A36, 37G10, 37G05.

Key words and phrases. Fold–Saddle singularity, canard, limit cycle, bifurcation, non–smooth vector field.

$\Omega^r = \Omega^r(K, f)$ the space of vector fields $Z : K \setminus \Sigma \rightarrow \mathbb{R}^2$ such that

$$Z(x, y) = \begin{cases} X(x, y), & \text{for } (x, y) \in \Sigma_+, \\ Y(x, y), & \text{for } (x, y) \in \Sigma_-, \end{cases}$$

where $X = (f_1, g_1)$, $Y = (f_2, g_2)$ are in χ^r . We write $Z = (X, Y)$, which we will accept to be multivalued in points of Σ . The trajectories of Z are solutions of $\dot{q} = Z(q)$, which has, in general, discontinuous right-hand side. The basic results of differential equations, in this context, were stated by Filippov in [2]. Related theories can be found in [4, 6, 8].

In what follows we will use the notation

$$X.f(p) = \langle \nabla f(p), X(p) \rangle \quad \text{and} \quad Y.f(p) = \langle \nabla f(p), Y(p) \rangle.$$

1.1. Setting the problem. Let X_0 be a smooth vector field defined in Σ_+ . We say that a point $p_0 \in \Sigma$ is a Σ -fold point of X_0 if $X_0.f(p_0) = 0$ but $X_0^2.f(p_0) \neq 0$. Moreover, $p_0 \in \Sigma$ is a *visible* (respectively *invisible*) Σ -fold point of X_0 if $X_0.f(p_0) = 0$ and $X_0^2.f(p_0) > 0$ (resp. $X_0^2.f(p_0) < 0$). In this universe, $\Gamma_{\Sigma}^{X_0}$, a Σ -fold point has codimension zero. Since $f(x, y) = y$ we derive the following generic normal forms $X_0(x, y) = (\alpha_1, \beta_1 x)$ with $\alpha_1 = \pm 1$ and $\beta_1 = \pm 1$.

Let Y_0 be a smooth vector field defined in Σ_- . Assume that Y_0 has a hyperbolic saddle point S_{Y_0} on Σ and that the eigenspaces of $DY_0(S_{Y_0})$ are transverse to Σ at S_{Y_0} . In this universe, $\Gamma_{\Sigma}^{Y_0}$, a saddle point S_{Y_0} has codimension one. Since $f(x, y) = y$ we derive the following generic normal forms $Y_0(x, y) = (\alpha_2 y, \alpha_2 x)$ with $\alpha_2 = \pm 1$ and its generic unfolding $Y_{\beta} = (\alpha_2(y + \beta), \alpha_2 x)$ where $\beta \in \mathbb{R}$. Let U be a small neighborhood of Y_0 in $\Gamma_{\Sigma}^{Y_0}$. Then:

- (a) There exists a smooth function $L : U \rightarrow \mathbb{R}$, such that DL_{Y_0} is surjective.
- (b) The correspondence $Y \rightarrow S_Y$ is smooth, where S_Y is a saddle point of Y .
- (c) If $L(Y) > 0$ then $S_Y \in \Sigma_-$.
- (d) If $L(Y) = 0$ then $S_Y \in \Sigma$.
- (e) If $L(Y) < 0$ then $S_Y \in \Sigma_+$.

In this paper we are concerned with the bifurcation diagram of systems $Z_0 = (X_0, Y_0)$ in Ω^r such that $p_0 = S_{Y_0} \in \Sigma$. This singularity will be called **Fold – Saddle** singularity (see Figures 1 and 2).

We depart from $Z_0^i, Z_0^v \in \Omega^r$ written in the following forms:

$$(1) \quad Z_0^i = \begin{cases} X_0^i = \begin{pmatrix} 1 \\ -x \end{pmatrix} & \text{if } y \geq 0, \\ Y_0 = \begin{pmatrix} -y \\ -x \end{pmatrix} & \text{if } y \leq 0, \text{ and} \end{cases}$$

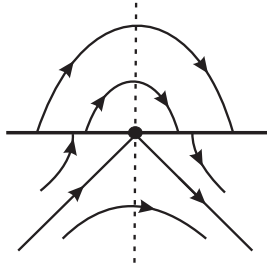


FIGURE 1. (Invisible) Fold-Saddle Singularity.

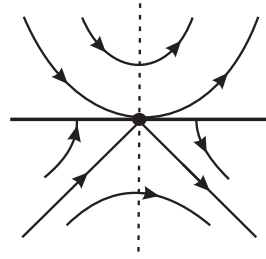


FIGURE 2. (Visible) Fold-Saddle Singularity.

$$(2) \quad Z_0^v = \begin{cases} X_0^v = \begin{pmatrix} 1 \\ x \end{pmatrix} & \text{if } y \geq 0, \\ Y_0 = \begin{pmatrix} -y \\ -x \end{pmatrix} & \text{if } y \leq 0. \end{cases}$$

Note that X_0^i presents an invisible Σ -fold point on its phase portrait and X_0^v presents a visible one. Following the techniques developed in [7], we are able to prove that there exists a smooth mapping $F_\tau : \Omega^r, Z_0^\tau \rightarrow \mathbb{R}^3, 0$ where $\tau = i$ or v such that:

1- $(DF_\tau)_{Z_0^\tau}$ is surjective (So $M_\tau = (F_\tau)^{-1}(0)$ is locally, around Z_0^τ , an imbedded differentiable manifold).

2- Each $Z \in U_\tau$, with $F_\tau(Z) = 0$ and U_τ a small neighborhood of Z_0^τ in Ω^r is C^0 -equivalent to Z_0^τ .

The main question is to exhibit the bifurcation diagram of Z_0^τ . So, we have to consider generic imbeddings $\sigma_\tau : \mathbb{R}^3, 0 \rightarrow \Omega^r, Z_0^\tau$ (3-parameter families). They are transversal imbeddings to M_τ at Z_0^τ .

Consider $Z_0^\tau = (X_0^\tau, Y_0) \in U_\tau$. Roughly speaking, we derive that:

I- There is a canonical imbedding $F_0^\tau : \mathbb{R}^2, 0 \rightarrow \chi^\tau, Z_0^\tau$ such that $F_0^\tau(\lambda, \beta) = Z_{\lambda, \beta}^\tau$ expressed by:

$$(3) \quad Z_{\lambda, \beta}^\tau = \begin{cases} X_\lambda^\tau = \begin{pmatrix} 1 \\ \alpha_1(\tau)(x - \lambda) \end{pmatrix} & \text{if } y \geq 0, \\ Y_\beta = \begin{pmatrix} -(y + \beta) \\ -x \end{pmatrix} & \text{if } y \leq 0, \end{cases}$$

where $\lambda, \beta \in (-1, 1)$, $\alpha_1(i) = -1$ and $\alpha_1(v) = 1$. Moreover, its bifurcation diagram of $Z_{\lambda, \beta}^\tau$ is exhibited (see Figures 18 and 28). We observe that there are some typical topological types nearby Z_0^τ that do not appear in the bifurcation diagram of $Z_{\lambda, \beta}^\tau$. For example, when $\tau = i$ the configurations in Figures 3 and 4 are excluded and when $\tau = v$ the configuration in Figure 5 also is excluded.

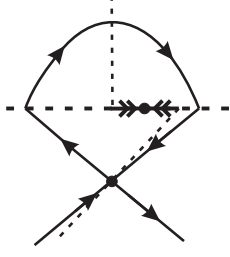


FIGURE 3.

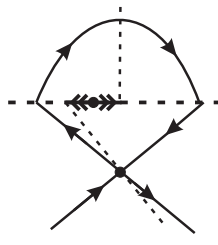


FIGURE 4.

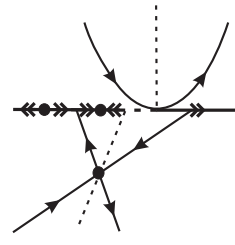


FIGURE 5.

II- We add an auxiliary parameter μ in the following way:

$$(4) \quad \bar{Z}_{\lambda,\mu,\beta}^{\tau} = \begin{cases} X_{\lambda} = \begin{pmatrix} 1 \\ \alpha_1(\tau)(x - \lambda) \end{pmatrix} & \text{if } y \geq 0, \\ Y_{\mu,\beta} = \begin{pmatrix} \frac{\mu}{2}x + \frac{(\mu-2)}{2}(y + \beta) \\ \frac{(\mu-2)}{2}x + \frac{\mu}{2}(y + \beta) \end{pmatrix} & \text{if } y \leq 0, \end{cases}$$

where $\lambda, \beta \in (-1, 1)$, $\alpha_1(i) = -1$, $\alpha_1(v) = 1$ and $\mu \in (-\varepsilon_0, \varepsilon_0)$ with the real number $\varepsilon_0 > 0$ being sufficiently small. By means of this late unfolding its bifurcation diagram cover all topological types near $\bar{Z}_{0,0,0}^{\tau}$.

In this universe, $\Gamma^{Z_0^{\tau}}$, a Fold–Saddle singularity has codimension three. Since $f(x, y) = y$ we derive the generic normal forms $\bar{Z}_{\lambda,\mu_0,\beta}^{\tau}$ with $\mu_0 = \pm\varepsilon_0/2$ and its generic unfolding $\bar{Z}_{\lambda,\mu,\beta}^{\tau}$ given by (4). Therefore, there is a codimension three bifurcation (global) branch terminating at Z_0^{τ} . In fact, note that we can obtain Equation (1) (respectively (2)) from Equation (4) taking $\tau = i$ (respectively $\tau = v$), $\lambda = 0$, $\mu = 0$ and $\beta = 0$.

Of course, we can take another generic normal form of one or both vector fields X_0 and Y_0 . In this paper we consider just the cases described in Equations (1) and (2). For the other cases a similar approach can be done.

It is worth mentioning that we detect branches of “canard cycles” in the bifurcation diagram of $\bar{Z}_{\lambda,\mu,\beta}^i$. Recall that, a canard cycle is a closed path composed by pieces of orbits of X , Y and Z^{Σ} (see Figures 7, 8 and 9). In Section 2 a precise definition will be given.

Example 1. Equations (1) and (2) appear in problems related to Control Theory, more specifically, in Relay Systems. In fact, consider the function $\varphi : \mathbb{R} \rightarrow \mathbb{R}$ given by

$$\varphi(y) = \begin{cases} -1, & \text{for } y \geq 0, \\ -y, & \text{for } y \leq 0, \end{cases}$$

and $u(y) = -\varphi(y)\text{sign}(y)$. So (1) and (2) are represented by $\tilde{Z}_0^{\tau}(x, y) = (u(y), \bar{\alpha}(\tau)x)$ where $\tau = i$ or v , $\bar{\alpha}(i) = -1$ and $\bar{\alpha}(v) = \text{sign}(y)$.

1.2. Statement of the Main Results. Our results are now stated. Theorems 1, 2 and 3 are intermediate steps towards Theorem A and Theorems 4, 5 and 6 are intermediate steps towards Theorem B.

Theorem 1. *Take $\tau = i$ in Equation (3) or equivalently, take $\tau = i$ and $\mu = 0$ in Equation (4). The (λ, β) -plane contains essentially 17 distinct typical configurations representing 5 distinct topological behaviors on its bifurcation diagram (see Figure 18).*

It is easy to see that the cases covered by Theorem 1 do not represent the full unfolding of the (Invisible) Fold–Saddle singularity. Because of this, the next two theorems are necessary. Each one of them describes a distinct generic codimension two singularity.

Theorem 2. *Take $\tau = i$ and $0 < \mu < \varepsilon_0$ in Equation (4). The (λ, β) -plane contains essentially 19 distinct typical configurations representing 7 distinct topological behaviors on its bifurcation diagram (see Figure 20).*

Theorem 3. *Take $\tau = i$ and $-\varepsilon_0 < \mu < 0$ in Equation (4). The (λ, β) -plane contains essentially 19 distinct typical configurations representing 7 distinct topological behaviors on its bifurcation diagram (see Figure 22).*

Theorem 4. *Take $\tau = v$ in Equation (3) or equivalently, take $\tau = v$ and $\mu = 0$ in Equation (4). The (λ, β) -plane contains essentially 13 distinct typical configurations representing 7 distinct topological behaviors on its bifurcation diagram (see Figure 28).*

The cases covered by Theorem 4 do not represent the full unfolding of the (Visible) Fold–Saddle singularity. Because of this, the next two theorems are necessary. Each one of them describes a distinct generic codimension two singularity.

Theorem 5. *Take $\tau = v$ and $0 < \mu < \varepsilon_0$ in Equation (4). The (λ, β) -plane contains essentially 13 distinct typical configurations representing 7 distinct topological behaviors on its bifurcation diagram (see Figure 28).*

Theorem 6. *Take $\tau = v$ and $-\varepsilon_0 < \mu < 0$ in Equation (4). The (λ, β) -plane contains essentially 13 distinct typical configurations representing 7 distinct topological behaviors on its bifurcation diagram (see Figure 28).*

Finally, we are able to state the main results of the paper.

Theorem A. *Equation (4) with $\tau = i$ generically unfolds the (Invisible) Fold–Saddle singularity. Moreover, its bifurcation diagram exhibits 55 distinct typical configurations representing 11 distinct topological behavior (see Figure 23).*

Theorem B. *Equation (4) with $\tau = v$ generically unfolds the (Visible) Fold–Saddle singularity. Moreover, its bifurcation diagram exhibits 39 distinct typical configurations representing 21 distinct topological behavior (see Figure 30).*

The paper is organized as follows: in Section 2 we give the basic theory about Non–Smooth Vector Fields on the Plane, in Section 3 we prove Theorem 1, in Section 4 we prove Theorem 2, in Section 5 we prove Theorem 3, in Section 6 we prove Theorem A and present the Bifurcation Diagram of $\overline{Z}_{\lambda,\mu,\beta}^i$, in Section 7 we prove Theorem 4, in Section 8 we prove Theorem 5, in Section 9 we prove Theorem 6 and in Section 10 we prove Theorem B and present the Bifurcation Diagram of $\overline{Z}_{\lambda,\mu,\beta}^v$.

2. PRELIMINARIES

We distinguish the following regions on the discontinuity set Σ :

- (i) $\Sigma_1 \subseteq \Sigma$ is the *sewing region* if $(X.f)(Y.f) > 0$ on Σ_1 .
- (ii) $\Sigma_2 \subseteq \Sigma$ is the *escaping region* if $(X.f) > 0$ and $(Y.f) < 0$ on Σ_2 .
- (iii) $\Sigma_3 \subseteq \Sigma$ is the *sliding region* if $(X.f) < 0$ and $(Y.f) > 0$ on Σ_3 .

Consider $Z \in \Omega^r$. The *sliding vector field* associated to Z is the vector field Z^s tangent to Σ_3 and defined at $q \in \Sigma_3$ by $Z^s(q) = m - q$ with m being the point where the segment joining $q + X(q)$ and $q + Y(q)$ is tangent to Σ_3 (see Figure 6). It is clear that if $q \in \Sigma_3$ then $q \in \Sigma_2$ for $-Z$ and then we can define the *escaping vector field* on Σ_2 associated to Z by $Z^e = -(-Z)^s$. In what follows we use the notation Z^Σ for both cases.

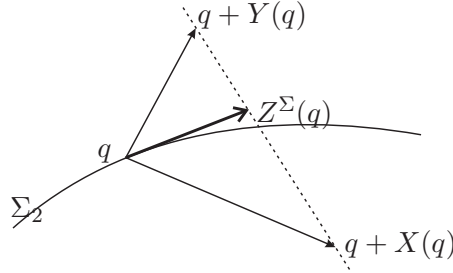


FIGURE 6. Fillipov's convention.

We say that $q \in \Sigma$ is a Σ –*regular point* if

- (i) $(X.f(q))(Y.f(q)) > 0$ or
- (ii) $(X.f(q))(Y.f(q)) < 0$ and $Z^\Sigma(q) \neq 0$ (that is $q \in \Sigma_2 \cup \Sigma_3$ and it is not a singular point of Z^Σ).

The points of Σ which are not Σ –*regular* are called Σ –*singular*. We distinguish two subsets in the set of Σ –*singular* points: Σ^t and Σ^p . Any $q \in \Sigma^p$

is called a *pseudo equilibrium* of Z and it is characterized by $Z^\Sigma(q) = 0$. Any $q \in \Sigma^t$ is called a *tangential singularity* and is characterized by $Z^\Sigma(q) \neq 0$ and $X.f(q)Y.f(q) = 0$ (q is a contact point of Z^Σ).

A pseudo equilibrium $q \in \Sigma^p$ is a Σ -*saddle* provided one of the following condition is satisfied: (i) $q \in \Sigma_2$ and q is an attractor for Z^Σ or (ii) $q \in \Sigma_3$ and q is a repeller for Z^Σ . A pseudo equilibrium $q \in \Sigma^p$ is a Σ -*repeller* (resp. Σ -*attractor*) provided $q \in \Sigma_2$ (resp. $q \in \Sigma_3$) and q is a repeller (resp. attractor) equilibrium point for Z^Σ .

Definition 1. Consider $Z \in \Omega^r$.

- (1) A curve Γ is a **canard cycle** if Γ is closed and
 - Γ contains arcs of at least two of the vector fields $X|_{\Sigma_+}$, $Y|_{\Sigma_-}$ and Z^Σ or is composed by a single arc of Z^Σ ;
 - the transition between arcs of X and arcs of Y happens in sewing points;
 - the transition between arcs of X (or Y) and arcs of Z^Σ happens through Σ -fold points or regular points in the escape or sliding arc, respecting the orientation. Moreover if $\Gamma \neq \Sigma$ then there exists at least one visible Σ -fold point on each connected component of $\Gamma \cap \Sigma$.
- (2) Let Γ be a canard cycle of Z . We say that
 - Γ is a **canard cycle of kind I** if Γ meets Σ just in sewing points;
 - Γ is a **canard cycle of kind II** se $\Gamma = \Sigma$;
 - Γ is a **canard cycle of kind III** if Γ contains at least one visible Σ -fold point of Z .

In Figures 7, 8 and 9 arise canard cycles of kind I, II and III respectively.
- (3) Let Γ be a canard cycle. We say that Γ is **hyperbolic** if
 - Γ is of kind I and $\eta'(p) \neq 1$, where η is the first return map defined on a segment T with $p \in T \cap \gamma$;
 - Γ is of kind II;
 - Γ is of kind III and or $\Gamma \cap \Sigma \subseteq \Sigma_1 \cup \Sigma_2$ or $\Gamma \cap \Sigma \subseteq \Sigma_1 \cup \Sigma_3$.

Remark 1. The expression “canard” is used here because these orbits are limit periodic sets of singular perturbation problems (see [1]).

Definition 2. Consider $Z \in \Omega^r$. A point $q \in \Sigma$ is a Σ -**center** if there is a neighborhood U of q such that an one parameter family of canard cycles encircles q and foliates U .

Definition 3. Consider $Z \in \Omega^r$. A closed path Δ is a Σ -**graph** if it is a union of equilibria, pseudo equilibria, tangential singularities of Z and arcs of Z joining these points in such a way that $\Delta \cap \Sigma \neq \emptyset$. Like for canard

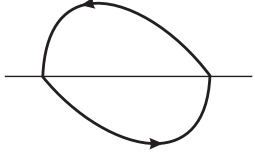


FIGURE
7. Canard
cycle of
kind I.

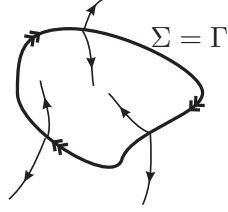


FIGURE
8. Canard
cycle of
kind II.

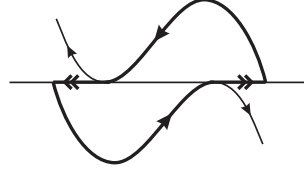


FIGURE
9. Canard
cycle of kind
III.

cycles, we say that Δ is a Σ -graph of kind I if $\Delta \cap \Sigma \subset \Sigma_1$, Δ is a Σ -graph of kind II if $\Delta \cap \Sigma = \Delta$ and Δ is a Σ -graph of kind III if $\Delta \cap \Sigma \subsetneq \Sigma_2 \cup \Sigma_3$.

In what follows, in order to simplify the calculations, we take $\mu = \alpha + 1$ in (4) and obtain the following expression

$$(5) \quad Z_{\lambda, \alpha, \beta}^T = \begin{cases} X_\lambda = \begin{pmatrix} 1 \\ \alpha_1(\tau)(x - \lambda) \end{pmatrix} & \text{if } y \geq 0, \\ Y_{\alpha, \beta} = \begin{pmatrix} \frac{(1+\alpha)}{2}x + \frac{(-1+\alpha)}{2}(y + \beta) \\ \frac{(-1+\alpha)}{2}x + \frac{(1+\alpha)}{2}(y + \beta) \end{pmatrix} & \text{if } y \leq 0, \end{cases}$$

where $\lambda, \beta \in (-1, 1)$, $\alpha \in (-1 - \varepsilon_0, -1 + \varepsilon_0)$, $\tau = i$ or v , $\alpha_1(i) = -1$ and $\alpha_1(v) = 1$. When it does not produce confusion, in order to simplify the notation we use $Z = (X, Y)$ or $Z_{\lambda, \alpha, \beta} = (X, Y)$ instead $Z_{\lambda, \alpha, \beta}^T = (X_\lambda, Y_{\alpha, \beta})$.

Given $Z = (X, Y)$, we describe some properties of both $X = X_\lambda$ and $Y = Y_{\alpha, \beta}$.

The real number λ measures how the Σ -fold point $d = (\lambda, 0)$ of X is translated away from the origin. More specifically, if $\lambda < 0$ then d is translated to the left hand side and if $\lambda > 0$ then d is translated to the right hand side.

Some calculations show that the curve $Y.f = 0$ is given by $y = \frac{(1-\alpha)}{(1+\alpha)}x - \beta$. So the points of this curve are equidistant from the separatrices when $\alpha = -1$. It become closer to the stable separatrix of the saddle point $S = S_{\alpha, \beta}$ when $\alpha \in (-1, -1 + \varepsilon_0)$. It become closer to the unstable separatrix of S when $\alpha \in (-1 - \varepsilon_0, -1)$. Moreover, the smooth vector field Y has distinct types of contact with Σ according with the particular deformation considered. In this way, we have to consider the following behaviors:

- \mathbf{Y}^- : In this case $\beta < 0$. So S is translated to the y -direction with $y > 0$ (and S is not visible for Z). It has a visible Σ -fold point $e = e_{\alpha, \beta} = \left(\frac{(1+\alpha)}{(1-\alpha)}\beta, 0 \right)$ (see Figure 10).
- \mathbf{Y}^0 : In this case $\beta = 0$. So S is not translated (see Figure 1).

- \mathbf{Y}^+ : In this case $\beta > 0$. So S is translated to the y -direction with $y < 0$. It has an invisible Σ -fold point $i = (i_1, i_2) = i_{\alpha, \beta} = \left(\frac{(1+\alpha)}{(1-\alpha)}\beta, 0\right)$. Moreover, we distinguish two points: $h = h_\beta = (-\beta, 0)$ which is the intersection between the unstable separatrix with Σ and $j = j_\beta = (\beta, 0)$ which is the intersection between the stable separatrix with Σ (see Figure 11).

In Figure 11 we distinguish the arcs σ_1 of Y joining the saddle point S of Y to h and σ_2 of Y joining j to the saddle point S of Y .

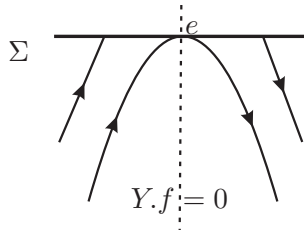


FIGURE 10. Case Y^- .

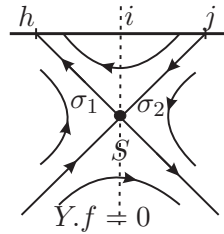


FIGURE 11. Case Y^+ .

3. PROOF OF THEOREM 1

In $(a, b) \subset \Sigma_2 \cup \Sigma_3$, consider the point $c = (c_1, c_2)$, the vectors $X(c) = (d_1, d_2)$ and $Y(c) = (e_1, e_2)$ (as illustrated in Figure 12). The straight segment passing through $c + X(c)$ and $c + Y(c)$ meets Σ in a point $p(c)$. We define the C^r -map

$$p : (a, b) \longrightarrow \Sigma$$

$$z \longmapsto p(z).$$

We can choose local coordinates such that Σ is the x -axis; so $c = (c_1, 0)$ and $p(c) \in \mathbb{R} \times \{0\}$ can be identified with points in \mathbb{R} . According with this identification, the *direction function* on Σ is defined by

$$H : (a, b) \longrightarrow \mathbb{R}$$

$$z \longmapsto p(z) - z.$$

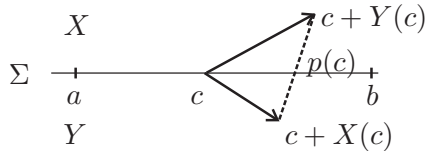


FIGURE 12. Direction function.

We obtain that H is a C^r -map and

- if $H(c) < 0$ then the orientation of Z^Σ in a small neighborhood of c is from b to a ;

- if $H(c) = 0$ then $c \in \Sigma^p$;
- if $H(c) > 0$ then the orientation of Z^Σ in a small neighborhood of c is from a to b .

Simple calculations show that $p(c_1) = \frac{e_2(d_1+c_1)-d_2(e_1+c_1)}{e_2-d_2}$ and consequently,

$$(6) \quad H(c_1) = \frac{e_2d_1 - d_2e_1}{e_2 - d_2}.$$

We now in position to prove Theorem 1.

Proof of Theorem 1. In Cases 1_1 , 2_1 and 3_1 we assume that Y presents the behavior Y^- . In Cases 4_1 , 5_1 and 6_1 we assume that Y presents the behavior Y^0 . In these cases canard cycles are not allowed.

◊ *Case 1_1 .* $d < e$, *Case 2_1 .* $d = e$ and *Case 3_1 .* $d > e$: The points of Σ outside the interval (d, e) belong to Σ_1 . The points inside this interval, when it is not degenerated, belong to Σ_3 in Case 1_1 and to Σ_2 in Case 3_1 . In both cases $H(z) > 0$ for all $z \in (d, e)$. See Figure 13.

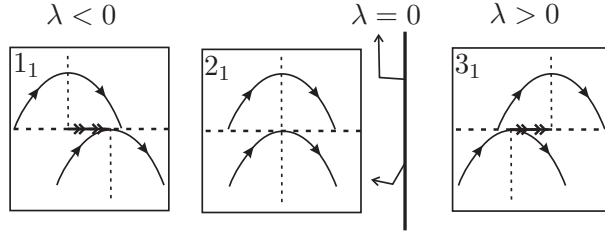


FIGURE 13. Cases 1_1 , 2_1 and 3_1 .

◊ *Case 4_1 .* $d < S$, *Case 5_1 .* $d = S$ and *Case 6_1 .* $d > S$: The points of Σ outside the interval (d, S) belong to Σ_1 . The points inside this interval, when it is not degenerated, belong to Σ_3 in Case 4_1 and to Σ_2 in Case 6_1 . In both cases $H(z) > 0$ for all $z \in (d, S)$. See Figure 14.

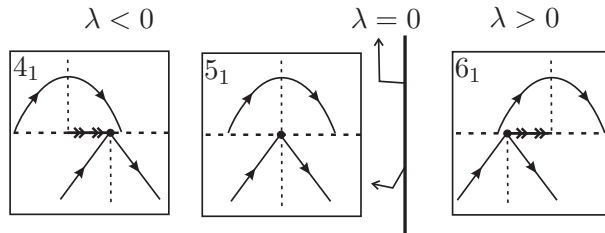


FIGURE 14. Cases 4_1 , 5_1 and 6_1 .

In Cases $7_1 - 17_1$ we assume that Y presents the behavior Y^+ .

◇ *Case 7₁*. $\lambda < -\beta$, *Case 8₁*. $\lambda = -\beta$, *Case 9₁*. $-\beta < \lambda < -\beta/2$, *Case 10₁*. $\lambda = -\beta/2$ and *Case 11₁*. $-\beta/2 < \lambda < 0$: The points of Σ outside the interval (d, i) belong to Σ_1 . The points inside this interval belong to Σ_3 . The direction function H assumes positive values in a neighborhood of d , negative values in a neighborhood of i and $H(\lambda\beta/(1 + \beta)) = 0$. So, by (6), the Σ -attractor $P = (\lambda\beta/(1 + \beta), 0)$, nearby $(0, 0)$, is the unique pseudo equilibrium. In these cases canard cycles are not allowed. See Figure 15.

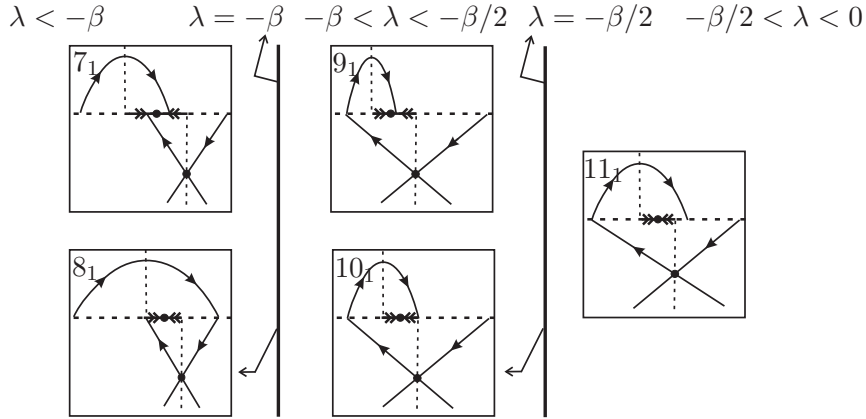


FIGURE 15. Cases 7₁ – 11₁.

◇ *Case 12₁*. $\lambda = 0$: Since $\alpha = -1$ and $d = i$, it is straightforward to show that each point $Q \in (h, i)$ belongs to a closed curve composed by an arc of X and an arc of Y . So $d = i$ is a Σ -center. See Figure 16.

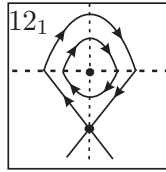


FIGURE 16. Case 12₁.

◇ *Case 13₁*. $0 < \lambda < \beta/2$, *Case 14₁*. $\lambda = \beta/2$, *Case 15₁*. $\beta/2 < \lambda < \beta$, *Case 16₁*. $\lambda = \beta$ and *Case 17₁*. $\lambda > \beta$: The points of Σ outside the interval (i, d) belong to Σ_1 and the points inside this interval belong to Σ_2 . The direction function H assumes positive values in a neighborhood of d , negative values in a neighborhood of i and $H(\lambda\beta/(1 + \beta)) = 0$. So, by (6), the Σ -repeller $P = (\lambda\beta/(1 + \beta), 0)$, nearby $(0, 0)$, is the unique pseudo equilibrium. In these cases canard cycles are not allowed. See Figure 17.

The bifurcation diagram is illustrated in Figure 18. □

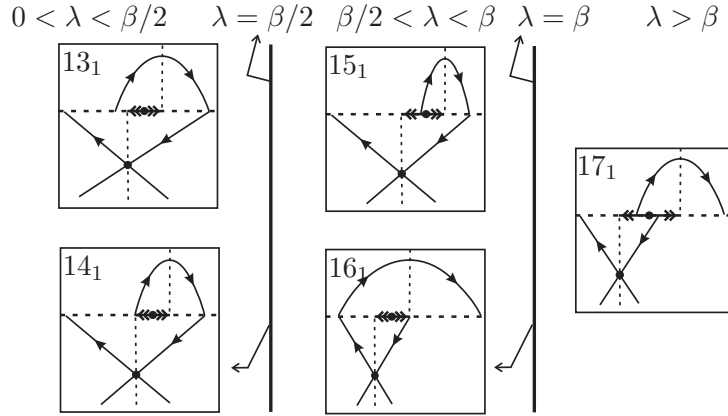
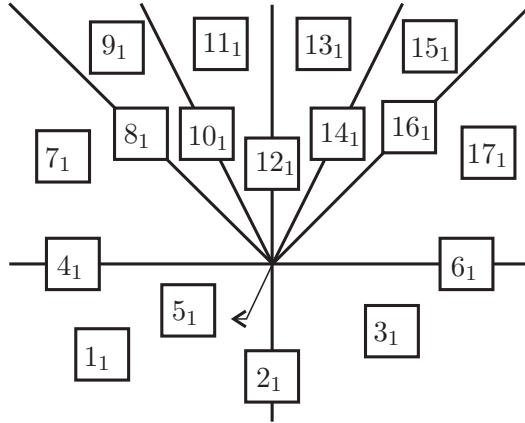
FIGURE 17. Cases $13_1 - 17_1$.

FIGURE 18. Bifurcation Diagram of Theorem 1.

4. PROOF OF THEOREM 2

Proof of Theorem 2. In Cases 1_2 , 2_2 and 3_2 we assume that Y presents the behavior Y^- . In Cases 4_2 , 5_2 and 6_2 we assume that Y presents the behavior Y^0 . In Cases $7_2 - 19_2$ we assume that Y presents the behavior Y^+ .

◊ *Case 1_2 .* $d < e$, *Case 2_2 .* $d = e$, *Case 3_2 .* $d > e$, *Case 4_2 .* $d < S$, *Case 5_2 .* $d = S$ and *Case 6_2 .* $d > S$: Analogous to Cases 1_1 , 2_1 , 3_1 , 4_1 , 5_1 and 6_1 .

◊ *Case 7_2 .* $\lambda < -\beta$, *Case 8_2 .* $\lambda = -\beta$, *Case 9_2 .* $-\beta < \lambda < -\beta/(1 - \alpha)$, *Case 10_2 .* $\lambda = -\beta/(1 - \alpha)$ and *Case 11_2 .* $-\beta/(1 - \alpha) < \lambda < 0$: Analogous to Cases $7_1 - 11_1$ changing $-\beta/2$ by $-\beta/(1 - \alpha) = -\text{dist}(h, i)/2$, where $\text{dist}(h, i)$ is the distance between h and i . The unique pseudo equilibrium

occurs in $P = (p^-, 0)$ where

$$(7) \quad p^- = \frac{1}{2(\alpha + 1)} \left(((1 - \alpha)(1 + \beta) + \lambda(1 + \alpha)) + \sqrt{((1 - \alpha)(1 + \beta) + \lambda(1 + \alpha))^2 - 4\beta(1 + \alpha)(1 + \alpha + \lambda(1 - \alpha))} \right).$$

◊ *Case 12₂*. $\lambda = 0$: The points of Σ outside the interval (d, i) belong to Σ_1 and the points inside this interval belong to Σ_3 . The direction function H assumes positive values in a neighborhood of d , negative values in a neighborhood of i and $H(p_0^+, 0) = 0$ where p_0^+ is given by (7) with $\lambda = 0$. So $P = (p_0^+, 0)$ is a Σ -attractor. Since $e = 0$, it is easy to see that there is an arc γ_1^X of X connecting the points h and j . It generates a Σ -graph $\Gamma = \gamma_1^X \cup \sigma_2 \cup S \cup \sigma_1$ of kind I. Since $-1 < \alpha < -1 + \varepsilon_0$, it is straight forward to show that the *First Return Map* $\eta = \varphi_Y \circ \varphi_X$, where

$$\begin{aligned} \varphi_X : \quad \Sigma &\rightarrow \Sigma \\ z = (x, 0) &\mapsto (-x + 2\lambda, 0) \quad \text{and} \\ \varphi_Y : \quad (i, j) \subset \Sigma &\rightarrow (h, i) \subset \Sigma \\ z = (x, 0) &\mapsto \left(\frac{x(i_1 + \beta) - 2i_1^2}{\beta - i_1}, 0 \right), \end{aligned}$$

has derivative bigger than 1 in the interval (h, d) . By consequence, Γ is a repeller for the trajectories inside it and in this case canard cycles are not allowed. See Figure 19.

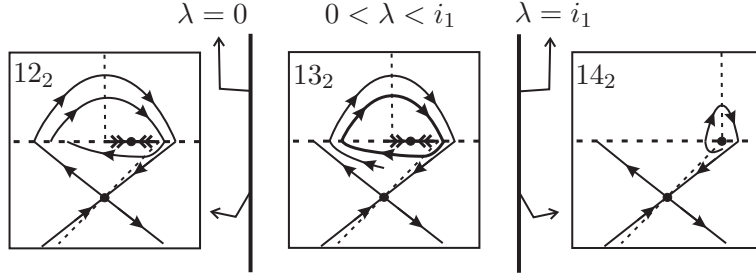


FIGURE 19. Cases 12₂, 13₂ and 14₂.

◊ *Case 13₂*. $0 < \lambda < i_1$: The distribution of the connected components of Σ and the behavior of H are the same of Case 12₂ with $P = (p_\lambda^+, 0)$ where p_λ^+ is given by (7). Since $0 < \lambda < i_1$, there is an arc γ_1^X of X connecting the point j to a point $k_1 \in (h, d)$. Also there is an arc γ_1^Y of Y connecting the point k_1 to a point $l_1 \in (i, j)$. Repeating this argument, we can find an increasing sequence $(k_i)_{i \in \mathbb{N}}$. We can prove that there is an interval $I \subset (k_1, d)$ such that $\eta' = (\varphi_Y \circ \varphi_X)' < 1$. As P is a Σ -attractor, there is an interval $J \subset (k_1, d)$ such that $\eta' > 1$. Moreover, there exists an

unique point $Q \in (k_1, d)$ given by $Q = ((-i_1^2 + \lambda(i_1 + \beta))/\beta, 0)$ such that $\eta' = 1$. By Q passes a repeller canard cycle Γ of kind I. See Figure 19.

◊ *Case 14₂*. $\lambda = i_1$: Every point of Σ belongs to Σ_1 except the point $d = i$. As in the previous case, we can construct sequences $(k_i)_{i \in \mathbb{N}}$ and $(l_i)_{i \in \mathbb{N}}$. Since $e = i_1$, we have that $k_i \rightarrow d$ and $l_i \rightarrow d$. So d is a non generic tangential singularity of repeller kind. In this case canard cycles are not allowed. See Figure 19.

◊ *Case 15₂*. $i_1 < \lambda < \alpha\beta/(1 - \alpha)$, *Case 16₂*. $\lambda = \alpha\beta/(1 - \alpha)$, *Case 17₂*. $\alpha\beta/(1 - \alpha) < \lambda < \beta$, *Case 18₂*. $\lambda = \beta$ and *Case 19₂*. $\lambda > \beta$: Analogous to Cases 13₁ – 17₁ changing $\beta/2$ by $\alpha\beta/(1 - \alpha) = -dist(i, j)/2$. The unique pseudo equilibrium occurs in $P = (p^-, 0)$ where p^- is given by (7).

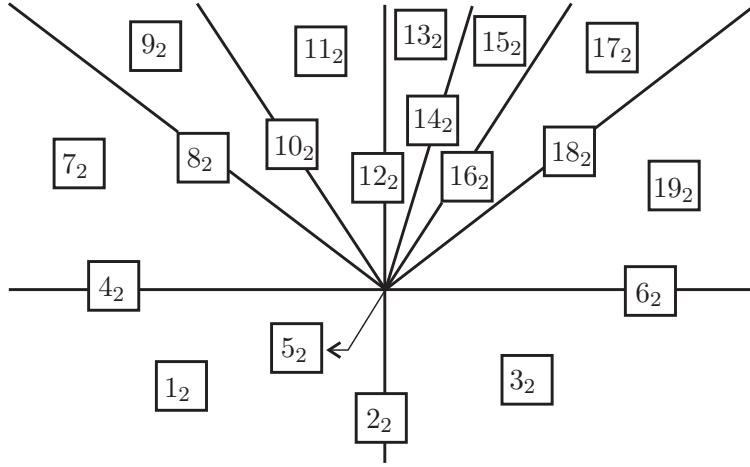


FIGURE 20. Bifurcation Diagram of Theorem 2.

The bifurcation diagram is illustrated in Figure 20. □

5. PROOF OF THEOREM 3

Proof of Theorem 3. In Cases 1₃, 2₃ and 3₃ we assume that Y presents the behavior Y^- . In Cases 4₃, 5₃ and 6₃ we assume that Y presents the behavior Y^0 . In Cases 7₃ – 19₃ we assume that Y presents the behavior Y^+ .

◊ *Case 1₃*. $d < e$, *Case 2₃*. $d = e$, *Case 3₃*. $d > e$, *Case 4₃*. $d < S$, *Case 5₃*. $d = S$ and *Case 6₃*. $d > S$: Analogous to Cases 1₁, 2₁, 3₁, 4₁, 5₁ and 6₁.

◊ *Case 7₃*. $\lambda < -\beta$, *Case 8₃*. $\lambda = -\beta$, *Case 9₃*. $-\beta < \lambda < -\beta/(1 - \alpha)$, *Case 10₃*. $\lambda = -\beta/(1 - \alpha)$ and *Case 11₃*. $-\beta/(1 - \alpha) < \lambda < i_1$: Analogous to Cases 7₁ – 11₁ changing $-\beta/2$ by $-\beta/(1 - \alpha) = -dist(h, i)/2$. The unique pseudo equilibrium occurs in $P = (p^-, 0)$ where p^- is given by (7).

◊ *Case 12₃*. $\lambda = i_1$: Analogous to Case 14₂ except that here d is an attractor, i.e., there is a change of stability. See Figure 21.

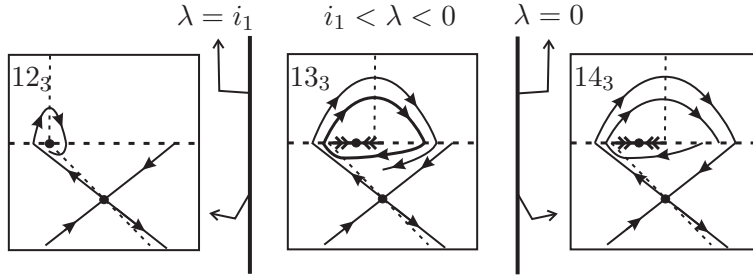


FIGURE 21. Cases 12_3 , 13_3 and 14_3 .

◊ *Case 13_3 .* $i_1 < \lambda < 0$: Analogous to Case 13_2 except that there is a change of stability on $P = (p^-, 0)$, which is a Σ -repeller, and on Γ , which is an attractor canard cycle of kind I. See Figure 21.

◊ *Case 14_3 .* $\lambda = 0$: Analogous to Case 12_2 except that occurs a change of stability on $P = (p^-, 0)$, which is a Σ -repeller, and on Γ , which is an attractor for the trajectories inside it. See Figure 21.

◊ *Case 15_3 .* $0 < \lambda < \alpha\beta/(1 - \alpha)$, *Case 16_3 .* $\lambda = \alpha\beta/(1 - \alpha)$, *Case 17_3 .* $\alpha\beta/(1 - \alpha) < \lambda < \beta$, *Case 18_3 .* $\lambda = \beta$ and *Case 19_2 .* $\lambda > \beta$: Analogous to Cases $13_1 - 17_1$ changing $\beta/2$ by $\alpha\beta/(1 - \alpha) = -dist(i, j)/2$. The unique pseudo equilibrium occurs in $P = (p^-, 0)$.

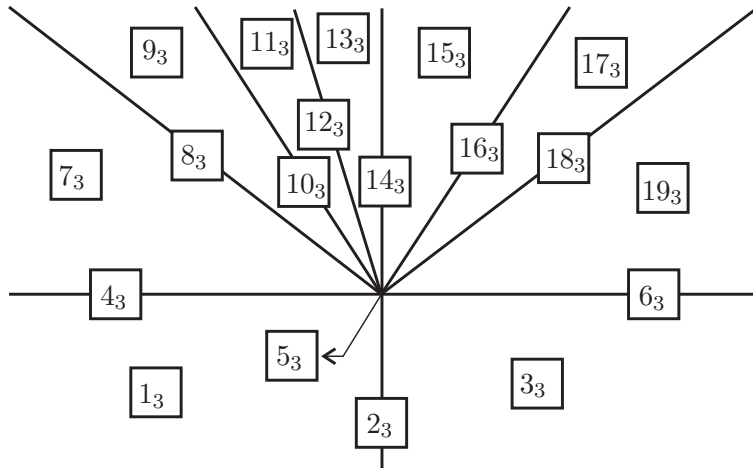


FIGURE 22. Bifurcation Diagram of Theorem 3.

The bifurcation diagram is illustrated in Figure 22.

□

6. PROOF OF THEOREM A

Proof of Theorem A. Since in Equation (5) we can take α in the interval $(-\infty, 0)$, from Theorems 1, 2 and 3 we derive that this equation, with $\tau = i$, unfolds generically the (Invisible) Fold–Saddle singularity.

Observe that the bifurcation diagram contain all the typical configurations and all the distinct topological behavior described in Theorems 1, 2 and 3. So, the number of typical configurations is 55 and the number of distinct topological behaviors is 11. Moreover, each topological behavior can be represented respectively by the Cases $1_1, 4_1, 7_1, 12_1, 13_1, 12_2, 13_2, 14_2, 12_3, 13_3$ and 14_3 .

The full behavior of the three–parameter family of non–smooth vector fields presenting the normal form (5), with $\tau = i$, is illustrated in Figure 23 where we consider a sphere around the point $(\lambda, \mu, \beta) = (0, 0, 0)$ with a small ray and so we make a stereographic projection defined on the entire sphere, except the south pole. Still in relation with this figure, the numbers pictured correspond to the occurrence of the cases described in the previous theorems. As expected, the cases 5_1 and 5_2 are not represented in this figure because they are, respectively, the center and the south pole of the sphere. \square

7. PROOF OF THEOREM 4

Proof of Theorem 4. Since X has a unique Σ –fold point which is visible we conclude that canard cycles are not allowed.

In Cases $1_4, 2_4$ and 3_4 we assume that Y presents the behavior Y^- . In Cases $4_4, 5_4$ and 6_4 we assume that Y presents the behavior Y^0 . In these cases, when it is well defined, the direction function H assumes positive values.

\diamond *Case 1_4 .* $d < e$: The points of Σ inside the interval (d, e) belong to Σ_1 . The points on the left of d belong to Σ_3 and the points on the right of e belong to Σ_2 . See Figure 24.

\diamond *Case 2_4 .* $d = e$: Here $\Sigma_1 = \emptyset$. The vector fields X and Y are linearly dependent on $d = e$ which is a tangential singularity. Moreover, it is an attractor for the trajectories of Z crossing Σ_3 and a repeller for the trajectories of Z crossing Σ_2 . See Figure 24.

\diamond *Case 3_4 .* $d > e$: The points of Σ inside the interval (e, d) belong to Σ_1 . The points on the left of e belong to Σ_3 and the points on the right of d belong to Σ_2 . See Figure 24.

\diamond *Case 4_4 .* $d < S$: The points of Σ inside the interval (d, S) belong to Σ_1 . The points on the left of d belong to Σ_3 and the points on the right of S belong to Σ_2 . See Figure 25.

\diamond *Case 5_4 .* $d = S$: Here $\Sigma_1 = \emptyset$ and S is an attractor for the trajectories of Z crossing Σ_3 and it is a repeller for the trajectories of Z crossing Σ_2 . See Figure 25.

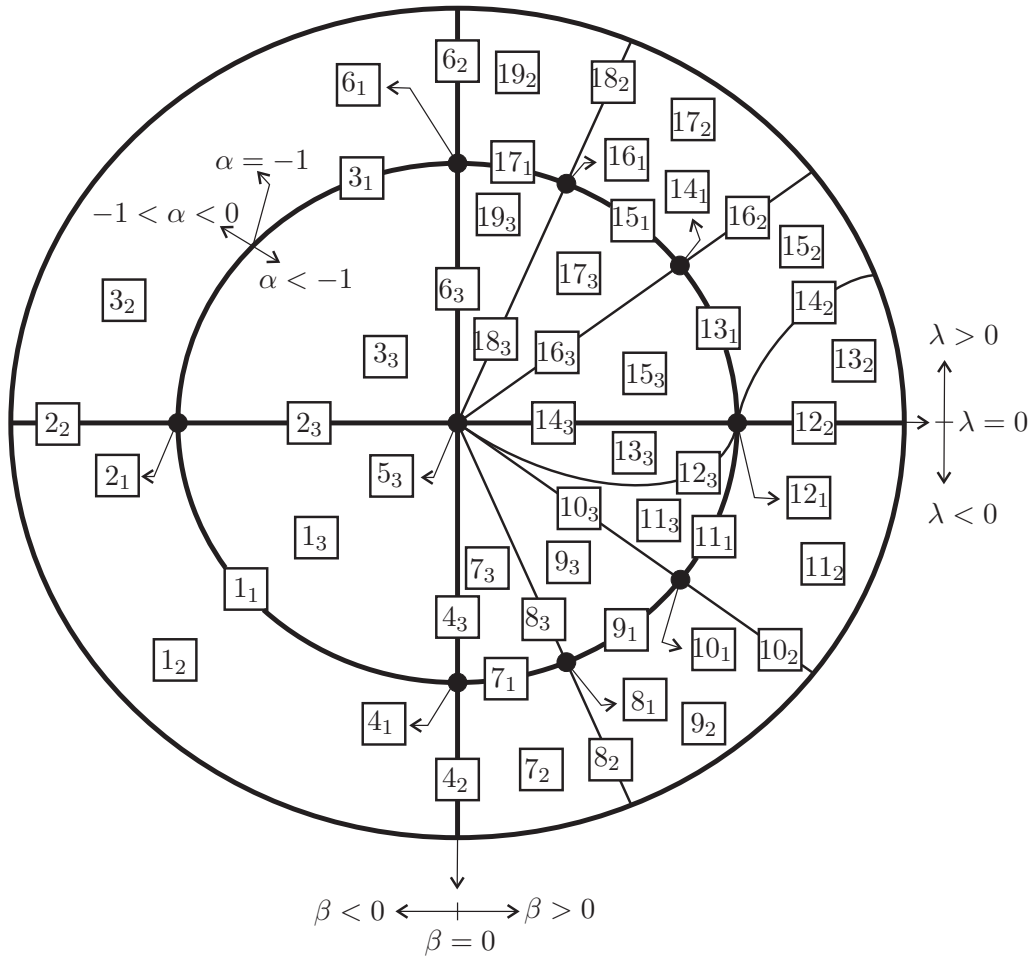


FIGURE 23. Bifurcation diagram of the (Invisible) Fold-Saddle singularity.

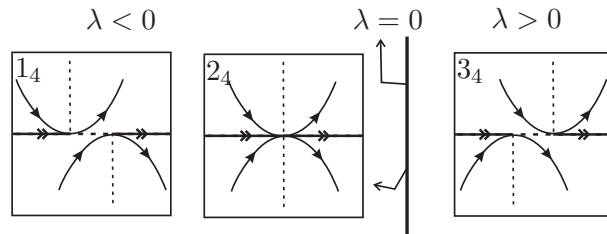
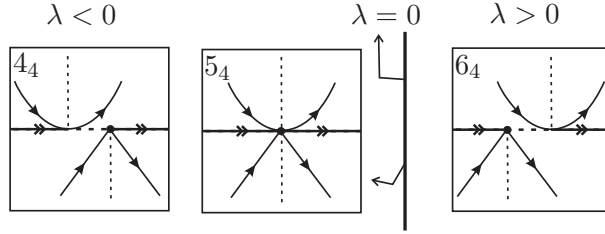


FIGURE 24. Cases 1₄, 2₄ and 3₄.

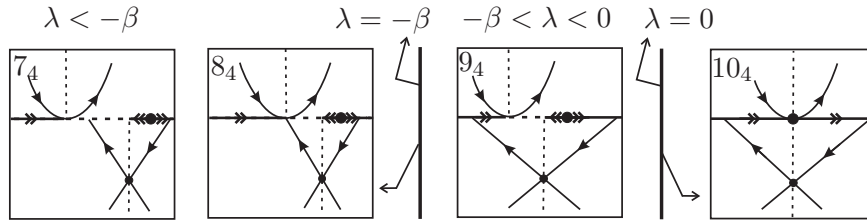
◇ *Case 6₄. $d > S$:* The points of Σ inside the interval (d, S) belong to Σ_1 . The points on the left of S belong to Σ_3 and the points on the right of d belong to Σ_2 . See Figure 25.

FIGURE 25. Cases 4_4 , 5_4 and 6_4 .

In Cases $7_4 - 13_4$ we assume that Y presents the behavior Y^+ .

◊ *Case 7_4 .* $d < h$, *Case 8_4 .* $d = h$ and *Case 9_4 .* $h < d < i$: The points of Σ inside the interval (d, i) belong to Σ_1 . The points on the left of d belong to Σ_3 and the points on the right of i belong to Σ_2 . The direction function H assumes positive values on Σ_3 and negative values in a neighborhood of i . Moreover, $H(\beta\lambda/(-1+\beta)) = 0$ and the Σ -repeller $P = (\beta\lambda/(-1+\beta), 0)$ is the unique pseudo equilibrium. See Figure 26.

◊ *Case 10_4 .* $d = i$: Here $\Sigma_1 = \emptyset$. The vector fields X and Y are linearly dependent on the tangential singularity $d = i$. A straightforward calculation shows that $H(z) = (1-\beta)/2 \neq 0$ for all $z \in \Sigma/\{d\}$. So $d = i$ is an attractor for the trajectories of Z crossing Σ_3 and a repeller for the trajectories of Z crossing Σ_2 . Moreover, $\Delta = \{d\} \cup \overline{d} \cup \sigma_2 \cup \{S\} \cup \sigma_1 \cup \overline{hd}$ is a Σ -graph of kind III in such a way that each Q in its interior belongs to another Σ -graph of kind III passing through d . See Figure 26.

FIGURE 26. Cases $7_4 - 10_4$.

◊ *Case 11_4 .* $i < d < j$, *Case 12_4 .* $d = j$ and *Case 13_4 .* $j < d$: The points of Σ inside the interval (i, d) belong to Σ_1 . The points on the left of i belong to Σ_3 and the points on the right of d belong to Σ_2 . The direction function H assumes positive values on Σ_2 and negative values in a neighborhood of i . Moreover, $H(\beta\lambda/(-1+\beta)) = 0$ and the Σ -attractor $P = (\beta\lambda/(-1+\beta), 0)$ is the unique pseudo equilibrium. See Figure 27.

The bifurcation diagram is illustrated in Figure 28. Each topological behavior can be represented respectively by Cases 1_4 , 2_4 , 4_4 , 5_4 , 7_4 , 10_4 and 11_4 . \square

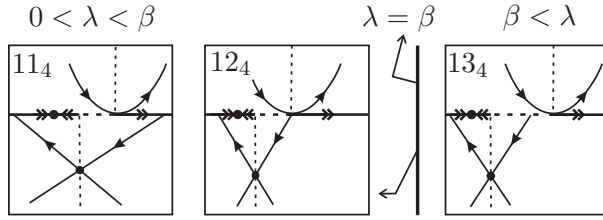


FIGURE 27. Cases $11_4 - 13_4$.

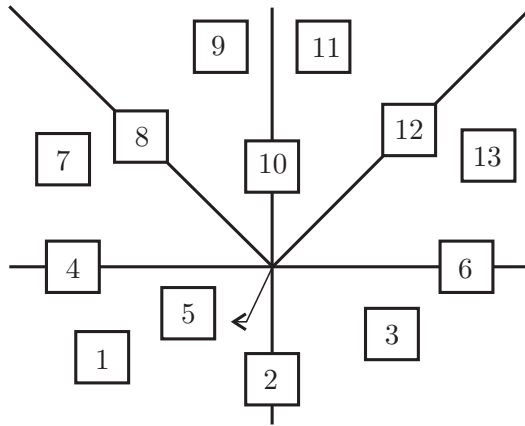


FIGURE 28. Bifurcation Diagram of Theorems 4, 5 and 6.

8. PROOF OF THEOREM 5

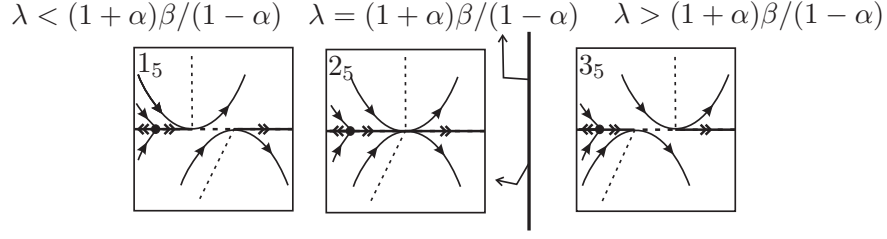
Proof of Theorem 5. The direction function H has a root $Q = (q, 0)$ where (8)

$$q = \frac{1}{2(\alpha + 1)} \left((-1 + \alpha)(1 - \beta) - \lambda(1 + \alpha) + \sqrt{((-1 + \alpha)(1 - \beta) - \lambda(1 + \alpha))^2 + 4\beta(1 + \alpha)(1 + \alpha + \lambda(-1 + \alpha))} \right).$$

Moreover, H assumes positive values on the right of Q and negative values on the left of Q . Note that when $\alpha \rightarrow -1$ so $Q \rightarrow -\infty$ under the line $\{y = 0\}$ and it occurs the configurations showed in Theorem 4.

In Cases $1_5, 2_5$ and 3_5 we assume that Y presents the behavior Y^- . In Cases $4_5, 5_5$ and 6_5 we assume that Y presents the behavior Y^0 . In Cases $7_5 - 13_5$ we assume that Y presents the behavior Y^+ .

◊ *Case 1_5 .* $d < e$, *Case 2_5 .* $d = e$, *Case 3_5 .* $d > e$, *Case 4_5 .* $d < S$, *Case 5_5 .* $d = S$ and *Case 6_5 .* $d > S$: Analogous to Cases $1_4, 2_4, 3_4, 4_4, 5_4$ and 6_4 respectively, except that here it appears the Σ -saddle Q on the left of d and e or S . See Figure 29.

FIGURE 29. Cases 1_5 , 2_5 and 3_5 .

◊ *Case 7_5 . $d < h$, Case 8_5 . $d = h$, Case 9_5 . $h < d < i$:* Analogous to Cases $7_4 - 9_4$, except that here it appears the Σ -saddle Q on the left of d and i . Here $P = (p, 0)$ where

(9)

$$p = \frac{1}{2(\alpha + 1)} \left((-1 + \alpha)(1 - \beta) - \lambda(1 + \alpha) + \sqrt{((-1 + \alpha)(1 - \beta) - \lambda(1 + \alpha))^2 + 4\beta(1 + \alpha)(1 + \alpha + \lambda(-1 + \alpha))} \right).$$

◊ *Case 10_5 . $d = i$:* Analogous to Case 10_4 , except that here appear the Σ -saddle Q on the left of $d = i$.

◊ *Case 11_5 . $i < d < j$, Case 12_5 . $d = j$ and Case 13_5 . $j < d$:* Analogous to Cases $11_4 - 13_4$, except that here it appears the Σ -saddle Q on the left of d and i .

The bifurcation diagram is illustrated in Figure 28. Each topological behavior can be represented respectively by Cases 1_5 , 2_5 , 4_5 , 5_5 , 7_5 , 10_5 and 11_5 . \square

9. PROOF OF THEOREM 6

Proof of Theorem 6. The direction function H has a root $Q = (q, 0)$ where q is given by (8). Moreover, H assumes positive values on the left of Q and negative values on the right of Q . Note that when $\alpha \rightarrow -1$ so $Q \rightarrow \infty$ under the line $\{y = 0\}$ and it occurs the configurations showed in Theorem 4.

◊ *Case 1_6 . $d < e$, Case 2_6 . $d = e$, Case 3_6 . $d > e$, Case 4_6 . $d < S$, Case 5_6 . $d = S$ and Case 6_6 . $d > S$, Case 7_6 . $d < h$, Case 8_6 . $d = h$, Case 9_6 . $h < d < i$, Case 10_6 . $d = i$, Case 11_6 . $i < d < j$, Case 12_6 . $d = j$ and Case 13_6 . $j < d$:* Analogous to Cases 1_5 , 2_5 , 3_5 , 4_5 , 5_5 , 6_5 , 7_5 , 8_5 , 9_5 , 10_5 , 11_5 , 12_5 and 13_5 respectively, except that here the Σ -saddle Q takes place on the right of d , e , S and i when these points appear.

The bifurcation diagram is illustrated in Figure 28. Each topological behavior can be represented respectively by Cases 1_6 , 2_6 , 4_6 , 5_6 , 7_6 , 10_6 and 11_6 . \square

10. PROOF OF THEOREM B

Proof of Theorem B. Since in Equation (5) we can take α in the interval $(-1 - \varepsilon_0, -1 + \varepsilon_0)$ we conclude that Theorems 4, 5 and 6 prove that this equation, with $\tau = v$, unfolds generically the (Visible) Fold-Saddle singularity. Its bifurcation diagram contains all typical configurations and all distinct topological behavior described in Theorems 4, 5 and 6. So, the number of typical configurations is 39 and the number of distinct topological behavior is 21. Moreover, each topological behavior can be represented respectively by the Cases $1_4, 1_5, 1_6, 2_4, 2_5, 2_6, 4_4, 4_5, 4_6, 5_4, 5_5, 5_6, 7_4, 7_5, 7_6, 10_4, 10_5, 10_6, 11_4, 11_5$ and 11_6 .

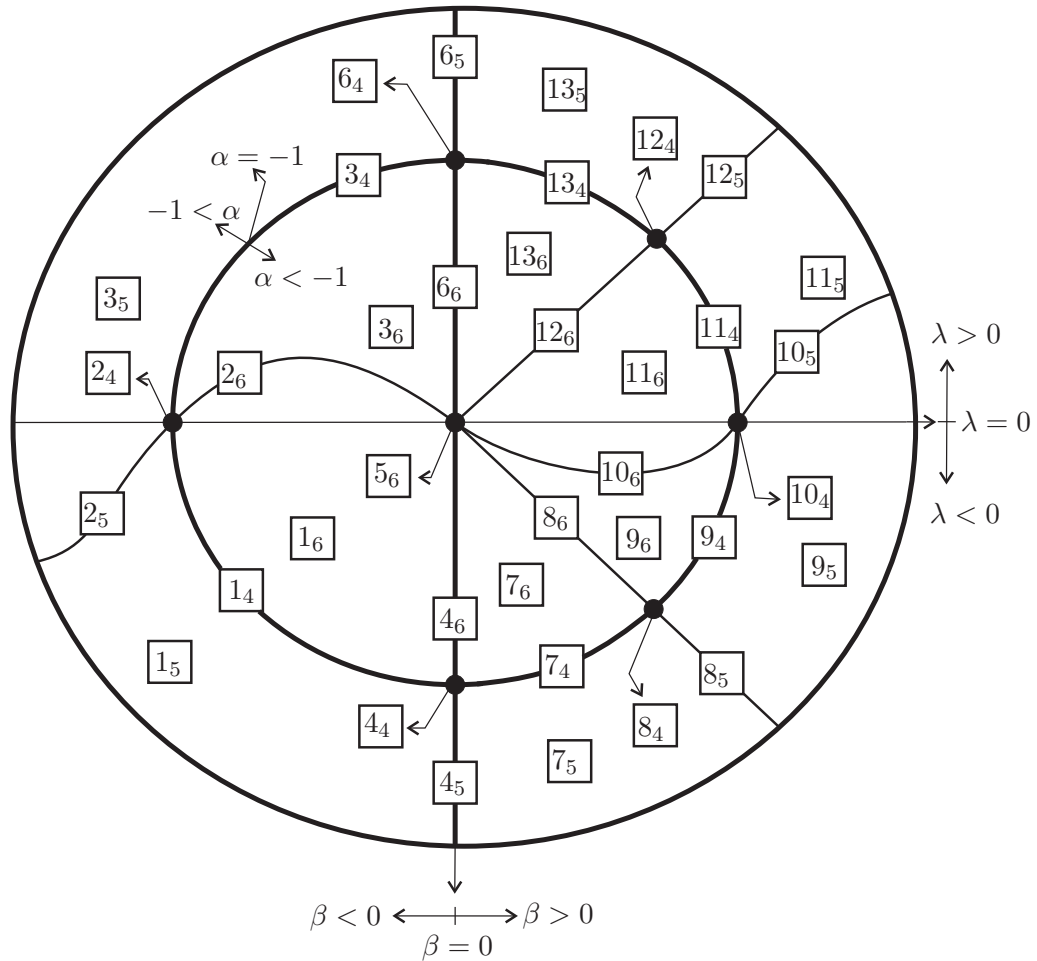


FIGURE 30. Bifurcation diagram of the (Visible) Fold-Saddle singularity.

The full behavior of the three-parameter family of non-smooth vector fields presenting the normal form (5), with $\tau = v$, is illustrated in Figure

30 where we consider a sphere around the point $(\lambda, \mu, \beta) = (0, 0, 0)$ with a small ray and so we make a stereographic projection defined on the entire sphere, except the south pole. Still in relation with this figure, the numbers pictured correspond to the occurrence of the cases described in the previous theorems. As expected, the cases 5_4 and 5_5 are not represented in this figure because they are, respectively, the center and the south pole of the sphere. \square

Acknowledgments. The first and the third authors are partially supported by a FAPESP-BRAZIL grant 2007/06896-5. The second author is partially supported by a FAPESP-BRAZIL grant 2007/08707-5.

REFERENCES

- [1] C.A. BUZZI, T. DE CARVALHO AND P.R. DA SILVA, *Canard Cycles and Poincaré Index of Non-Smooth Vector Fields on the Plane*, posted in arXiv:1002.4169v1 [math.DS].
- [2] A.F. FILIPPOV, *Differential Equations with Discontinuous Righthand Sides*, Mathematics and its Applications (Soviet Series), Kluwer Academic Publishers-Dordrecht, 1988.
- [3] M. GUARDIA, T.M. SEARA AND M.A. TEIXEIRA, *Generic bifurcations of low codimension of planar Filippov Systems*, posted in http://www.ma.utexas.edu/mp_arc-bin/mpa?yn=09-195.
- [4] V. S. KOZLOVA, *Roughness of a Discontinuous System*, Vestnik Moskovskogo Universiteta, Matematika **5** (1984), 16–20.
- [5] YU.A. KUZNETSOV, S. RINALDI AND A. GRAGNANI, *One-Parameter Bifurcations in Planar Filippov Systems*, Int. Journal of Bifurcation and Chaos, **13** (2003), 2157–2188.
- [6] J. SOTOMAYOR AND M.A. TEIXEIRA, *Regularization of Discontinuous Vector Fields*, International Conference on Differential Equations, Lisboa (1996), 207–223.
- [7] M.A. TEIXEIRA, *Generic Bifurcation in Manifolds with Boundary*, Journal of Differential Equations **25** (1977), 65–88.
- [8] M.A. TEIXEIRA, *Generic Singularities of Discontinuous Vector Fields*, An. Ac. Bras. Cienc. **53** (1991), 257–260.

¹ IBILCE–UNESP, CEP 15054–000, S. J. RIO PRETO, SÃO PAULO, BRAZIL

² IMECC–UNICAMP, CEP 13081–970, CAMPINAS, SÃO PAULO, BRAZIL

E-mail address: `buzzi@ibilce.unesp.br`

E-mail address: `tiago@ibilce.unesp.br`

E-mail address: `teixeira@ime.unicamp.br`